MECHANICAL ENGINEERING AND SOLID MECHANICS SERIES

RELIABILITY OF MULTIPHYSICAL SYSTEMS SET

Volume 9

Applications and Metrology at Nanometer Scale 1

Smart Materials, Electromagnetic Waves and Uncertainties

Pierre Richard Dahoo
Philippe Pougnet
Abdelkhalak El Hami

iSTE

WILEY

Applications and Metrology at Nanometer Scale 1

Reliability of Multiphysical Systems Set

coordinated by
Abdelkhalak El Hami

Volume 9

Applications and Metrology at Nanometer Scale 1

Smart Materials, Electromagnetic Waves and Uncertainties

Pierre-Richard Dahoo
Philippe Pougnet
Abdelkhalak El Hami

iSTE

WILEY

First published 2021 in Great Britain and the United States by ISTE Ltd and John Wiley & Sons, Inc.

ISTE Ltd
27-37 St George's Road
London SW19 4EU
UK

www.iste.co.uk

John Wiley & Sons, Inc.
111 River Street
Hoboken, NJ 07030
USA

www.wiley.com

Library of Congress Control Number: 2020946679

British Library Cataloguing-in-Publication Data
A CIP record for this book is available from the British Library
ISBN 978-1-78630-640-1

Contents

Preface

The various actions taken worldwide in support of sustainable development and greenhouse gas emission control have led to increasingly restrictive regulations. Manufacturers in the automotive field have thus developed innovative mechatronic systems, enabling various vehicle functions to go electric. Confronted with the globalization of exchanges that has generated stronger competition and a surge of new product performances, companies in the sector of embedded mechatronic systems are developing new products at an increasingly faster rate.

In other domains, to achieve volume or mass reduction or curb energy dissipation, manufacturers of mechatronic systems are developing new assembly methods based on multimaterials (e.g. composite materials, hybrids) or on innovative nanomaterials (e.g. carbon nanotubes). Modeling is essential to reduce product development cost, shrink time to market, understand failure mechanisms occurring in the operating conditions and optimize design before launching production. The reliability-based design optimization (RBDO) method is a modeling approach that optimizes design, guarantees the required high level of performance and takes into account the variability in the manufacturing process as well as the climatic variability in the use conditions. The efficiency of RBDO, however, depends on a solid understanding of the failure mechanisms caused by aging.

Creating a model of a dynamic system often involves developing a simplified model of its behavior based on realistic hypotheses and on the key parameters that are required for its functioning. The dynamic behavior of this modeled system is ruled by partial differential equations (PDEs). The model is then improved by introducing elements or parameters that were not

initially included and by improving the set of PDEs (nonlinearity, coupling, etc.), in order to obtain a model that closely represents the reality of operating systems and provides pertinent simulation results.

The theoretical models that are based on the fundamental laws of physics use a *bottom-up* approach. These models can be studied using analytical or numerical methods. When experiments can be implemented, simulation results are compared to experimental results. It is also possible to use experimental methods and a *top-down* approach to build a database of the response of the system to applied stresses. These data are then analyzed by comparing them to the response of theoretical or empirical models. In all the cases, there is a degree of uncertainty in the statistical analysis of the data, which leads to predictions with a margin of error. The lower the margin of error, the closer the predictions are to reality, leading to a sound understanding of the functionalities of working materials.

As Book 9 of the "Reliability of Multiphysical Systems Set", this book is designed to provide applications for Book 2 in the set, entitled *Nanometer-scale Defect Detection Using Polarized Light*. This is achieved by describing the experimental and theoretical methods developed in fundamental research laboratories to understand the physics or chemical processes, which at the nanometer scale are at the origin of the remarkable properties of the materials introduced in innovative technological devices. It presents optical techniques based on polarized light, which are used to characterize interface and bulk material defects that have an impact on the performance of nanodevices. It also describes how mechanical properties of nanomaterials can be determined using theoretical models and by the analysis of experimental results and their uncertainties.

This book is intended for students at master and doctoral levels, teaching academics and researchers in materials science, physics engineering and experimental study, as well as R&D and manufacturing engineers of large groups and SMEs in the field of electronics, mechatronics, or optical or electronic materials.

Chapter 1 provides a historical overview of the development of nanosciences and nanotechnologies and describes the challenges encountered when working on the nanometric scale, such as finding new ways to measure the physical properties of nanomaterials. It provides an overview of the techniques used for manufacturing nanomaterials: spin

coating, cathode sputtering and laser ablation. Four characterization and failure analysis techniques adapted to nanotechnologies are presented: transmission electron microscopy (TEM), scanning electron microscopy (SEM), atomic force microscopy (AFM) and attenuated total reflection (ATR) infrared spectroscopy.

Chapter 2 describes how to manage system variable uncertainties in the design process. The objective is to obtain a design that meets the performance requirements, has a stable response when design parameters vary randomly and respects a threshold of minimal performance for a given confidence level. Several methods for analyzing the effect on the output of uncertainties in the system input parameters are presented with practical applications: a probabilistic approach, interval analysis, a fuzzy logic method, designs of experiments and principal component analysis.

Chapter 3 is dedicated to various applications of electromagnetic waves. After a quick summary of the main characteristics of electromagnetic waves and microwave antenna theory, the following applications are studied: energy of a monochromatic plane wave, properties of a rectangular waveguide, performance of a wire antenna and antenna networks. These applications facilitate the understanding of the operation of antennas for the fifth generation (5G) of mobile telecommunication systems.

Chapter 4 deals with functional materials employed in intelligent systems. The main characteristic of these intelligent materials is the coupling of their various physical properties. Thermodynamic coupling and multiphysics coupling are studied for piezoelectric, magnetostrictive and shape memory materials. Application exercises are provided for the deformations of a plate-like thin layer, a piezoelectric accelerometer, a piezoelectric transducer and a piezoelectric sensor.

Pierre Richard DAHOO
Philippe POUGNET
Abdelkhalak EL HAMI
October 2020

Introduction

The scientific study of measurement is known as metrology. Any measure is based on a universally accepted standard and any measuring process is prone to uncertainty. In engineering science, measurement concerns various types of parameters. Legal metrology is imposed by a regulatory framework that the manufactured product must respect. Technical or scientific metrology involves the methods used to measure the technical characteristics of the manufactured product. In engineering sciences, measurement concerns various types of parameters. In a more general context of a systemic approach, metrology should also be considered in connection with other indicators of the production system. These measures enable the follow-up and development of the processes implemented for ensuring and optimizing product quality or reducing failure so that it meets client expectations. The ability of a product to meet quality and reliability expectations can be addressed in the design stage, according to a RBDO (Reliability-Based Design Optimization) approach described in the "Reliability of Multiphysical Systems Set Book 2", entitled *Nanometer-scale Defect Detection Using Polarized Light*. More generally, RBDO makes it possible to consider the uncertain parameters of manufacturing processes, measurement and operational conditions in order to optimize the manufacturing process, the design parameters and the overall quality of the product.

Reliability of Multiphysical Systems Set Book 2 focused on three levels of design for manufacturing an industrial product:

– Numerical methods developed in engineering from mathematical models and theories in order to optimize product quality from its design

according to RBDO. This methodology is a source of applications in engineering science intended to address optimization problems in the industrial field.

– Experimental methods developed in fundamental research relying on the light–matter interaction and on simulation-based analysis using theoretical models in order to make nanometer-scale measurements and conduct the analysis. These methods are used in nanosciences for the elaboration of knowledge leading to nanotechnologies.

– Finally, the application of these two approaches in the example presented in Chapter 9 of Reliability of Multiphysical Systems Set Book 2 (*Nanometer-scale Defect Detection Using Polarized Light*) to the measurement of the physical properties of a nanomaterial, carbon nanotube.

In sciences, there are various ways to measure a dimension. The measuring instruments or methods employed depend on the scale at which metrology is approached. In order to describe the issues at stake for measurement at a given scale, we present the methods employed for the measurement processes at two scales of interest for scientists, namely the infinitely small, which corresponds to the Planck length of 1.6×10^{-35} m, and the infinitely large, which corresponds to the diameter of the Universe evaluated at 8.8×10^{26} m. This is to help the reader understand that, even though becoming an expert in a scientific field or in a given subject is not the objective, it is necessary to understand some basic tenets in order to master the methods used for successful metrology at a given scale.

In 1899, Planck determined a unit of length $l_P = \sqrt{(Gh/2\pi c^3)} \approx 1.6 \times 10^{-35}$ m, referred to as Planck length, based on fundamental constants: G, gravitational constant (6.6×10^{-11} Nm^2 Kg^{-2}), h, Planck's constant (6.64×10^{-34} Js) and c, the speed of light ($2.99{,}729{,}458 \times 10^8$ ms^{-1}). This length cannot be measured with the measurement technologies available on Earth. Indeed, the smallest length measurable at the LHC (Large Hadron Collider) of CERN, the particle accelerator in which two protons are made to frontally collide in a ring of 26,659 km, which led to the discovery in 2012 of the Higgs boson, is approximately 10^{-16} m, which is 19 orders of magnitude higher than the Planck length. CMS and ATLAS detectors were used in the observation of the Higgs boson, the latest prediction of the standard model not yet observed. The measurement at the scale of 10^{-16} m is made by compressing energy to reach an infinitely small spatial volume.

The principle of measurement at the scale of fundamental particles is mainly based on three relations: the de Broglie relation between the momentum p and the wavelength λ, $p=h/\lambda$, which introduces the wave–particle duality for matter; the relation that links the energy E of a particle to its wave frequency or wavelength λ, such as proposed by Einstein to explain the photoelectric effect $E = hc/\lambda$; and the relation that links the energy E of a particle of rest mass m to its rest mass energy and to its kinetic energy associated with its momentum $p=mv$, $E^2= m^2c^4 + p^2c^2$, as mentioned in Einstein's special theory of relativity. In the above formulas, v is the speed of the particle of mass m and c is the speed of light. The energy E can also be expressed by the formula $E= \gamma mc^2$, where γ is given by $\gamma =1/\sqrt{(1-v^2/c^2)}$. The speed of a particle is therefore given by $v/c=\sqrt{(1-(mc^2/E)^2}$.

In the LHC, the energy of a proton is 7 TeV ($1.2\ 10^{-6}$ J), far higher (by a factor of 7,500) than its rest energy, mc^2, which is 938 MeV. The formula for speed can then be rewritten as $v/c = (1-(m^2c^4/2E^2))$, which is equal to 1 to the nearest 10^{-8}. Using the relation $E= hc/\lambda$, the resulting value of the wavelength is of the order of 10^{-16} m, which gives the dimensions that can be reached in the LHC. The mass measured during two experiments at CERN in the LHC (8 TeV in 2012 and 13 TeV in 2015) is confirmed to the value of 125 GeV.

To detect the Higgs boson, a particle of mass 125 GeV associated with the Higgs field, while the mass of a proton is 938 MeV, the proton is accelerated and consequently its kinetic energy is increased so that its energy given by $E= \gamma mc^2$ significantly exceeds 938 MeV (8 TeV in 2012 and 13 TeV in 2015). The disintegration of colliding protons, each contributing an energy load of 8 TeV or 13 TeV, releases sufficient energy so that the Higgs boson can be expected to emerge during the recombination of subatomic particles. As the Higgs boson decays quasi-instantaneously after its emergence, the products of its decay must be analyzed to identify the excess energy and therefore the excess mass about 125 GeV.

It is worth noting that at the Planck length, the required energies that cannot be expected in a particle accelerator would lead to the emergence of black holes.

The opposite dimensional extreme towards the infinitely large corresponds to the spatial extent of the Universe, whose estimated value according to cosmologists is 10^{26} m. In cosmology, the observable Universe is a term used to describe the visible part of our Universe, the point from which light reaches us. It is a sphere whose limit is located at the cosmological horizon, having the Earth at its center. It is therefore a relative notion, as for other observers located somewhere else in the Universe, the observable sphere would not be the same (while its radius would be identical).

In cosmology, distances are measured in light-years. A light-year is the distance that light travels in one year, which corresponds to approximately 9.5×10^{12} m. The megaparsec, which is 3.26 million (3.26×10^6) light-years, is another unit of distance that is also specific to extragalactic astrophysics. Finding the size of the Universe involves accurate measurements of fossil radiation, or of the cosmic microwave background (CMB) radiation that originated in the Big Bang and can be used to determine the volume filled by the Universe since its creation. Predicted for the first time by Ralph Alpher in 1948 in his thesis work, CMB was discovered by Arno Penzias and Robert Wilson at "Bell Telephone Laboratories" during the development of a new radio receiver following the interferences detected independently of the orientation of the antenna they were building. While in a first approximation CMB is isotropic, accurate measurements of this radiation lead to determining H_0, the Hubble constant, which indicates the rate of expansion of the Universe.

In cosmology, detectors are above-ground telescopes. The WMAP (Wilkinson Microwave Anisotropy Probe) satellite launched in 2001 enabled the detection of CMB with good accuracy. Its intensity varies slightly in different directions of the sky and the fluctuations can be determined. Extremely accurate measurements of the WMAP in 2003 made it possible to calculate a value of H_0 of 70 kilometers per second and per megaparsec, which is within 5% in the hypothesis of a constant rate of expansion. Since the Universe is accelerating, during its expansion, the correction brought to H_0 made it possible to estimate the age of the Universe to 13.75 billion years, with a 0.1 billion margin of error. It is the scale fitting the domain to which corresponds the age of the Universe deduced from observations related to the Big Bang based on the inflationary model in an expanding Universe.

After the Big Bang, the elementary subatomic particles had no mass and could travel at the speed of light. After the expansion of the Universe and its cooling, the particles interacted with the Higgs field and consequently gained a mass.

In the history of the Universe, the elementary particles interacted with the Higgs field, 10^{-12} s after the Big Bang. The value of 125 GeV is considered as the critical value between a stable universe and a metastable universe. The "standard model of cosmology" elaborated at the beginning of this century, towards 2000, is probably at present the best model that enables the description of the evolution of the Universe, the significant stages in the history of the observable Universe as well as its current content, as revealed by astronomical observations. The standard model describes the Universe as an expanding homogeneous and isotropic space, on which large structures are overlaid as a result of the gravitational collapse of primordial inhomogeneities, which were formed during the inflation phase. There are still questions to be addressed, such as the nature of certain constituents of the Universe, black matter, and black energy and their relative abundance.

The inflationary model relies on the hypothesis of the Universe expanding with an exponential acceleration $R(t)=R_0\exp(H(t)t)$, 10^{-30} s after the Big Bang, where $H(t)$ is the Hubble constant. This constant is measured from the Doppler effect, which explains the red shift of the light radiation emitted by a distant star that is receding from the point of observation. The inflationary model allows for a plausible interpretation of the CMB isotropy, with relative variations of the measured temperature of 10^{-5}. Based on the data provided by the Hubble, COBE (Cosmic Background Explorer**)** and WMAP (Wilkinson Microwave Anisotropy Probe) telescopes, as well as by the BOOMerang (Balloon Observations Of Millimetric Extragalactic Radiation ANd Geophysics) and MAXIMA (Millimeter Anisotropy eXperiment IMaging Array) experiments, scientists were able to determine the age of the Universe is 13.75 billion light-years.

The Universe is presently in accelerated expansion: if its speed is 70 km/s at 1 Megaparsec, it doubles at 2 Megaparsec, reaching 140 km/s and so on. Considering the Doppler shift or the red shift for the receding stars, and therefore the fact that not only are the stars receding, but also those that are twice farther recede twice faster, therefore considering the metrics applicable to the space that is stretching while galaxies are receding, the 13.8 billion years between the beginning of the rapid expansion of the Universe 10^{-30} s

after the Big Bang amount to 46.5 billion light-years, which is a radius of 93 billion light-years. Obviously, the light of stars that are at the periphery or at the cosmological horizon can no longer reach us, but as what we observe today goes back to the time needed for light to reach us while traveling a distance in a stretching space.

These two examples show that at each dimensional scale, besides the appropriate experimental measurement techniques required for observation, we must have a good mastery of the theories adapted for the interpretation and analysis of the gathered data. At each scale, the engineer must acquire specific knowledge elaborated in the laboratories and develop the competences to enable the mastery of technologies and the implementation of innovations.

This book which provides applications for Reliability of Multiphysical Systems Set Book 2 (*Nanometer-scale Defect Detection Using Polarized Light*), focuses on knowledge elaborated at the nanometer scale for applications in the field of engineering sciences. The subjects approached are related to simulation experiments and engineering of nanometer-scale systems. The light–matter interaction has a special place among the subjects addressed, because the analysis of the properties and characteristics of matter is most often possible due to light being used as a probe. Similarly, simulation according to theoretical models based on quantum mechanics principles requiring field theory is also given particular attention.

Nanotechnologies and nanosciences are identified as sources of breakthrough innovations that will lead to the development of technologies that are considered primordial in the 21st Century. They should be deployed in eco-innovations and will increasingly become pervasive in the societal applications in various sectors. Without pretending to provide an exhaustive list, several examples are worth being mentioned: new energies and their recovery and storage, water purification, new materials that are lighter and more resilient for land and space transportation, construction and buildings, information technologies with quantum computers, embedded electronic systems and factory 4.0. The trend according to which states throughout the world offer financial support for the development of long-term projects in this field dates back to the beginning of the 21st Century. This is a reflection of the economic growth potential in nanotechnologies.

Similar to the inflationary model proposed by cosmologists to explain the countless galaxies and planetary systems, suns and black holes that constitute them, there was also a sharp increase in the volume of activities in nanosciences. The subjects approached in this book and in the Reliability of Multiphysical Systems Set Book 2 (*Nanometer-scale Defect Detection Using Polarized Light*) concern the field of engineers working in mechatronics, robotics and computation in modeling and simulation, for the societal spin-offs of nanotechnologies in the fields of land and space transportation, handicap, information and simulation technologies in a systemic approach. The level of knowledge acquired by the engineer should make innovation in nanotechnologies possible.

The contents of *Nanometer-scale Defect Detection Using Polarized Light* and *Applications and Metrology at Nanometer Scale 1 & 2*, jointly written by three authors, aim to develop knowledge that is essential at the nanometer scale, enabling trainee-engineers or engineers to develop nanotechnology-based devices or systems. To promote the deployment of nanotechnologies, the authors of these three books whose joint competences and experiences associate know-how in fundamental physics, engineering sciences and industrial activities cover a wide spectrum of application domains. *Nanometer-scale Defect Detection Using Polarized Light* builds a theoretical and experimental basis for understanding nanometer-scale metrology. This book in two volumes, *Applications and Metrology at Nanometer Scale*, enriches this theoretical basis with applications in the form of corrected exercises.

1

Nanometer Scale

The methodologies implemented for the elaboration and analysis of materials or objects on the nanometer scale are part of nanotechnologies. The fundamental research conducted at this scale, which is referred to as nanoscience, generates knowledge on the innovative properties associated with nanometer dimensions, as well as on the relevant methods of analysis. Nanotechnologies concern technologies used for the industrial manufacturing of devices carrying a commercial and societal value, while following the safety limits applicable to nano-objects manipulation and use. It is essentially multidisciplinary and relies on chemistry, physics, materials science, simulation, information and communication technologies, engineering science and many other disciplines. Mechatronics and robotics for terrestrial and spatial transportations and the technologies for connected objects are concerned by the developments in nanotechnologies. Working at the nanometer scale requires especially adapted metrology, as measurements of the properties of nanodevices often lead to relative values whose standard deviation is of the same order of magnitude as the measured value. Indeed, in most cases, to qualify the measured values, simulations should be conducted in parallel with the measuring process.

1.1. Introduction

Historically, the landmark of the foundation of nanotechnology is the lecture given by R. Feynman, recipient of Nobel Prize for Physics in 1965 for his contribution to quantum electrodynamics. The lecture was entitled "There is plenty of room at the bottom", and was given on December 29, 1959, at the annual meeting of the American Physical Society at California

Applications and Metrology at Nanometer Scale 1:
Smart Materials, Electromagnetic Waves and Uncertainties,
First Edition. Pierre-Richard Dahoo, Philippe Pougnet and Abdelkhalak El Hami.

Institute of Technology. On this occasion, he stated: “The principles of physics, as far as I can see, are not against the possibility of manipulating things atom by atom”.

The term “nanotechnology” was coined by N. Taniguchi in 1974 [TAN 74], to describe the processes of thin-film deposition during the elaboration of “wafers” of semiconductors. The scanning electron microscope developed in 1981 [BIN 82a, BIN 82b, BIN 83 BIN 86a], for whose invention G. Binnig and H. Roher received the Nobel Prize for Physics in 1986, can be used to visualize surfaces at atomic or nanometer scale. In retrospect, some sort of Gant chart can be drawn to quantify the time lapse of over two decades between Feynman’s idea in 1959 on atom manipulation, the elaboration in the 1970s of materials or nano-objects structured at nanometer scale, including the invention of the term nanotechnology in 1974 and, finally, the development of the instrument enabling the effective visualization and manipulation of the atom, in 1981. Two major fields of investigation corresponding to different temporalities can be identified: a first phase for the controlled synthesis or elaboration of nano-objects, and a second phase for measurement and analysis. The acquisition of knowledge used by the engineer to implement innovations requires the development of imaging tools and especially of nanometer-scale analysis methods. The efficiency of the overall scientific effort depends on the availability of multidisciplinary competences, which involves a systemic approach.

Some of the most fascinating problems in all science fields involve multiple temporal or spatial scales (cosmology, materials science, elementary particles, etc.) so that in the science field, the scales of interest for scientists range from Planck length of 10^{-35} m to the distance of 10^{24} m, which, in cosmology, corresponds to the diameter of the volume of observation (local group) of the Universe since the Big Bang.

In the field of technologies and engineering sciences, the invention of the transistor in the 1950s by J. Bardeen and W. Brattain [BAR 48] and W. Shockley [SHO 49] of Bell Laboratories opened the way to micro-technologies. The integration density of transistors consequently doubled every two years, in accordance with Moore’s law [MOO 65]. As shown in Figure 1.1, the following stage of technology development is in the field of nanotechnologies, a source of innovations for the 21st-Century industry.

Figure 1.1 gives an overview of the various scales (on the X axis) that should be considered in materials sciences and in scientific subjects (quantum physics, chemistry, materials sciences and engineering) that elaborate the knowledge in the considered field (nanoscopic, microscopic, mesoscopic, macroscopic). The scale of interest for technological applications is naturally the macroscopic scale, the dimension perceived at human scale in society. The relations between material structure and properties determine the behavior of the material at the macroscopic scale. Figure 1.1 also indicates the properties or phenomena studied at various scales by simulation, providing a non-exhaustive list of several theoretical models developed for apprehending the behavior of the material (*ab initio* calculations, molecular dynamics, Monte Carlo simulation, dislocation dynamics and Monte Carlo dynamics, polycrystalline models, finite element method).

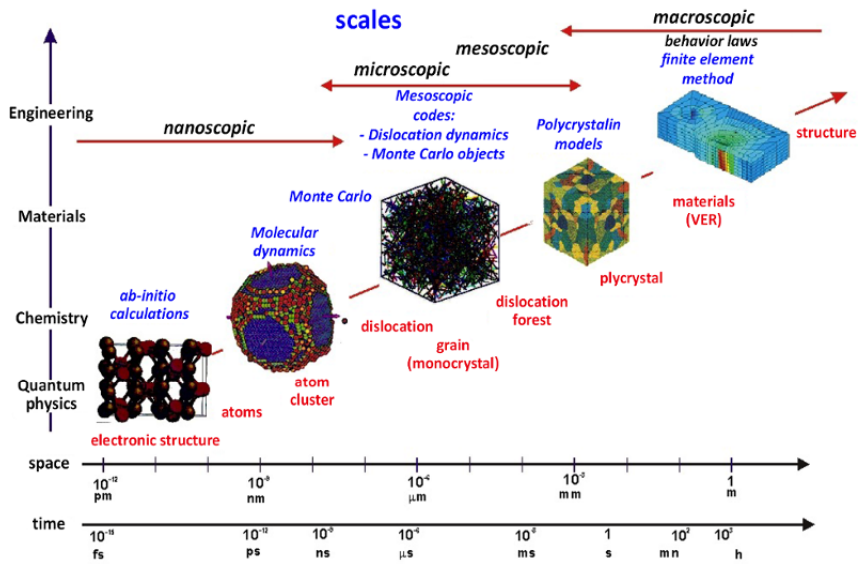

Figure 1.1. *Various spatial and temporal scales in materials sciences. For a color version of this figure, see www.iste.co.uk/dahoo/metrology1.zip*

The term nano originates in the Greek term "nannos" or "ναννοζ", which means "excessively short or dwarf". In metrology, which is the science of measurement, a nanometer corresponds to 10^{-9} m. While human hair size of 10^{-4} m is small on the meter scale, it is huge at the nanometer

scale. It is the scale corresponding to molecules. It was agreed to classify any object whose size ranges between 10^{-10} m and 10^{-7} m as belonging to the nanometer scale, though the term nano more generally describes measured dimensions that range between 1 nm and 100 nm. This interval contains, for example, dimensions corresponding to the size of viruses (100 nm), deoxyribonucleic acid or DNA (10 nm) and molecular structures (1 nm). The term nano generated a large number of terms whose prefix is nano. The terms employed in this book are mainly nanoscale, nanometric, nanosciences and nanotechnologies, thus referring the reader to works specifically dedicated to nanosciences and nanotechnologies.

Nanoresearch is conducted in many domains: nanoelectronics, modeling, simulation and design of nano-objects, nanobiotechnologies, nanomedicine, nanophotonics, nano-characterization, nanometrology, nanolithography, nano-fabrication of nano-objects, nanotoxicology in health, environment and nano-security fields. The knowledge and know-how related to all these domains can be found in numerous works that were published after the emergence of nanoscience in the 2000s. The readers who are interested in gaining in-depth knowledge in a specific field are referred to [RAT 02, LAH 04, DUP 06, LAH 06, LAH 07, LAH 10, LOU 16, KNE 20, LEE 20]. Being in continuous and rapid evolution in all the disciplines since 2000, nanoscience and nanotechnologies are the object of many calls for projects throughout the world.

On the nanometer scale, the classical theories of Newtonian mechanics are not adapted and the principles of quantum mechanics should be applied for the interpretation of the mechanics of physics and chemical phenomena. In classical mechanics, distant interactions are modeled by forces that act instantaneously throughout the space. While possible according to classical theory, simultaneous measurement of position and speed is not possible in quantum mechanics, following Heisenberg's uncertainty principle $\Delta x \Delta p \approx h/2\pi$, which must hold.

On the other hand, Maxwell's theory of the electromagnetic field, which is built in terms of electric and magnetic fields, is in agreement with the quantum description for matter–light interaction, as shown in [DAH 16].

In his works on the attraction of spheroids, Laplace shows that "the calculation with partial differences" can be used to locally formulate the interaction between two masses in terms of potentials. Laplace writes on

page 358 [LAP 94] that “a sphere attracts an external point as if all its mass were united in its center” and on page 382 [LAP 94] that “In the planetary theory, the objective is not to determine their equilibrium in absolute space, but only the equilibrium of all their parts around their centers of gravity”. Nevertheless, if gravitation is formulated in terms of fields or potential, as Laplace did in 1785 [LAP 94] to locally describe gravitational force, classical mechanics may be regarded as an approximation of the general theory of relativity. Unlike Maxwell formalism, which describes the electromagnetic phenomena in terms of electric and magnetic fields, it cannot be directly inserted in the quantum theory.

The transition from classical mechanics to QM is possible through the principle of correspondence between Poisson brackets defined in Hamiltonian mechanics and the commutators between operators acting in Hilbert space according to Heisenberg formalism. The formulation of the theory of gravitation in terms of gravitational fields as used in general relativity should be compared to the quantum field theory, which is more appropriate for the description of interactions between elementary particles.

All these considerations show that different formalisms were developed in order to describe the physical phenomena on various scales. To innovate in the field of nanotechnologies, the engineer should therefore apprehend and master the physical concepts that are currently being developed in research laboratories.

On the nanometer scale, implementing a technique for the measurement of a physical property is not a simple task, and when a measurement is made, its repeatability is not guaranteed. In general, in the absence of a standard as a reference, accuracy is hardly reached. And if precision is achievable, it requires a lot of time to be set up at the nanometer scale. Consequently, there are few measurements really achieved and the implementation of measurement instruments is not an easy task. Furthermore, measurements should also rely on theoretical models.

Experimental and theoretical examples for the study of materials at the nanometer scale are given in Chapter 6 of [DAH 16]. The first chapter of [DAH 16] provides an overview of the elaboration, characterization and analysis techniques relevant to nanotechnologies. There are two major fields of investigation in nanotechnologies, namely the synthesis or elaboration of nano-objects while controlling the manufacturing process and the process of

characterization and analysis, which involves the development of imaging and analysis tools at the nanometer scale. These studies rely on quantum mechanics principles.

Based on research works conducted in the laboratories of the University of Versailles as part of fundamental research [DAH 04a, DAH 04, FRA 05, HAM 06, HAM 07, NOU 07] or in relation with the industrial environment, three examples are considered to illustrate three techniques for the elaboration of nanomaterials samples: spin coating, cathode sputtering and laser ablation. Similarly, four techniques for sample study and characterization are presented: transmission electron microscope (TEM), scanning electron microscope (SEM), atomic force microscope (AFM) and ATR spectroscopy.

1.2. Sample elaboration

The samples studied in nanosciences are manufactured either in bulk form or as a thin film deposited on a substrate by chemical, physical and chemical or physic-chemical processes. A sample is classified as a nanomaterial if at least one of its dimensions ranges between 1 and 100 nm.

A thin film always involves a substrate, irrespective of the procedure employed for its manufacture (it may happen that a thin film is separated from its substrate). Consequently, the substrate has a very strong influence on the structural properties of the deposited film. The nature of the substrate influences the physical properties of a mono-material thin film, all other characteristics being the same. Thus, the physical properties of a thin film are slightly different depending on whether it is deposited on an amorphous insulating substrate, such as glass, or on a silicon monocrystalline substrate, for example. It is worth noting that a thin film is anisotropic by construction.

There are numerous methods for preparing thin films. Only those most commonly used in the field of electronics and technology in relation to transport, optics, magneto-optics and heat properties are mentioned here. The main manufacturing methodologies used by the manufacturers of active or passive electronic components are based on physical processes for the deposition of material on a substrate. Therefore, the thin film increases in thickness from zero and this growth must be controlled.

In the case of chemical deposition, the films grow through a chemical reaction between a substrate maintained at an optimal deposition temperature in the presence of an inert gas in a low pressure preparation chamber and a precursor fluid, which results in a solid film that covers the whole surface. Depending on the precursor phase, chemical deposition is differently classified. Some examples of coating are spin coating, dip coating, atomic layer deposition (ALD), electro-deposition and, finally, chemical vapor deposition (CVD), and the variants associated with CVD differ depending on the process used to initiate the chemical reactions and on the process conditions, such as plasma-enhanced (PECVD), metallo-organic (MOCVD) and very low-pressure CVD.

In the physical deposition processes, the material to be deposited is generated in solid, liquid or gaseous state, and then it is physically carried on the surface of the substrate. This stage takes place in a preparation chamber under vacuum. The processes through which the matter to be deposited is generated are essentially mechanical, thermal or electromechanical, such as thermal evaporation, sputtering or ion plating. The choice of the deposition process depends on a certain number of factors, such as the substrate structure, the deposition temperature, the deposition rate and the source of material. The deposited films can be structured by other techniques, such as photolithography.

Two large families of physical methods can be distinguished in practice. One of them involves a carrier gas that moves the material to be deposited from a recipient to the substrate and is related to scattering techniques used in the manufacture of active components. The other one involves a very low-pressure environment and the material to be deposited is carried by an initial thermal or mechanical pulse. To elaborate a thin film, we must choose the material to be deposited, the substrate and the deposition technique.

The three most common thin-film deposition techniques are cathode sputtering, molecular beam epitaxy and laser ablation.

– *Cathode sputtering*. A target is bombarded with an inert gas (argon) in order to sputter the atoms in the target. Applying a potential difference between the target (cathode) and the substrate (anode), the sputtered atoms are accelerated and deposited on the substrate.

– *Molecular beam epitaxy*. Conducted under high vacuum, this method involves the evaporation of the material to be deposited by heating, radiation or electron bombardment.

– *LASER ablation*. Groups of atoms in the target are "evaporated" by means of a high-fluence LASER beam.

Unlike magnetron or diode sputtering, which relies on a mechanical principle of atomic or more precisely ion bombardment, vacuum or ultra-high vacuum evaporation relies on a thermal principle. Heat brings matter to its melting point and then to its evaporation point.

Vacuum evaporation relies on two elementary processes, namely the evaporation of a heated source followed by condensation to solid state of the matter evaporated on the substrate. Matter heating can be generated by several techniques leading to its evaporation: Joule effect, through which a current of normally several hundred Amperes passes through the matter to evaporate, electron bombardment (evaporation using an electron gun), effusion evaporation, magnetron cathode sputtering, diode cathode sputtering and laser ablation evaporation.

Molecular beam epitaxy (MBE) is conducted under ultra-high vacuum. It involves the evaporation of the material to be deposited by heating, radiation or electron bombardment on a substrate. With this technique, one or several molecular beams of atoms can be directed towards the substrate to achieve epitaxial growth. It enables the growth of nano-structured samples of several cm^2 at a speed of about one atomic monolayer per second. An MBE setup consists of an introduction airlock equipped with a turbomolecular pump and a preparation chamber containing:

– a gun enabling ion bombardment of the surfaces (Ar+ ions of energy ranging between 1 and 8 keV);

– a furnace enabling heating up to 1,800°C by combining Joule effect up to 500°C and electron bombardment for temperatures beyond;

– a micro-leakage valve to introduce gas in the chamber. The temperature during growth is measured by a thermocouple and/or an infrared thermometer.

To illustrate the thin-film deposition techniques at nanometer scale, descriptions of spin coating, cathode sputtering and laser ablation techniques are detailed below.

1.2.1. *Physical and chemical method: spin coating*

One method for chemically preparing a polymer sample in the form of thin film on a substrate at nanoscale is spin coating. It is worth noting that there are several methods for preparing thin films, depending on the nature of the polymer, thickness and application, namely spin coating, dip coating or serigraphy.

This section presents the process used in a thesis work at the University of Versailles St Quentin, in a joint project with the transportation industry, funded within MOVEO, a competitiveness cluster [KHE 14]. The embedded electronics systems from car suppliers in the automotive industry comprise plastic materials, notably for coating electronic components. To ensure the reliability of the encapsulated devices, the quality of the plastic cases of the electronic components must be controlled. Due to their low costs and high performances, electronic cases are essentially made of plastic materials. In this respect, plastic cases are most often made from epoxy resin and silica. Water absorption is the first cause of deterioration of electronic cases, resulting in the formation of cracks and delaminations of the coating. Aging studies in humid or aqueous environments contribute to a better understanding of the various paths corresponding to physical or chemical degradations of resins. The presence of water more or less related to the polymer is identified as a main cause.

The study of interfaces at the nanometer scale was conducted on silicone gels used for the encapsulation of electronic circuits. These polysiloxane-based gels are polymers characterized by a silicon–carbon Si–C bond and by a silicon–oxygen Si–O bond. They are very stable at high temperatures ≥180°C and provide an electric insulation of 20 kV/mm, being both resistant to chemical products and moisture proof. The silica surface is characterized by the groups: silanols (Si–OH) and siloxanes (Si–O–Si). Interactions between the reactive functions of the polymer and the silanols of the silica surface are susceptible to appear at the silica surface. On the other hand, the presence of hydroxyl functions on the polymer chain supports the absorption and the fixation of the polymer by hydrogen bond to the surface of the silica particle. A coupling agent is added to modify the silica surface in order to favor the bonds between the organic polymer and the charges. It generally takes the form of an alkoxysilane. During the cross-linkage reaction, this agent forms stable chemical bonds between the polymer and the charges. One of the coupling agents that is currently used in the industry is

glycidyloxypropyltrimethoxysilane (GOTMS). The coupling agent can also be very useful at the interface between metal and resin, as it forms a hydrophobic film at the surface of the metal and enables a very good adhesion between the metal and the resin. The studied polymers were either single-component silicone gels or two-component silicone gels. The characterization of samples by ellipsometry at nanometer scale was presented in Chapter 8 of [DAH 16].

Spin coating is widely used for the deposition of polymer films on electronic components. It involves the deposition by a syringe of a given volume of polymer solution on the surface of a substrate. A vacuum pump enables the fixation by aspiration of the substrate on a rotary support during the rotation for the efficient spread of the film and a mechanical stability of the whole even at 10,000 rpm. The device spinner can reach a rotational speed of 10,000 rpm and an acceleration/deceleration from 1 to 7,500 rpm. The various stages are schematically represented in Figure 1.2.

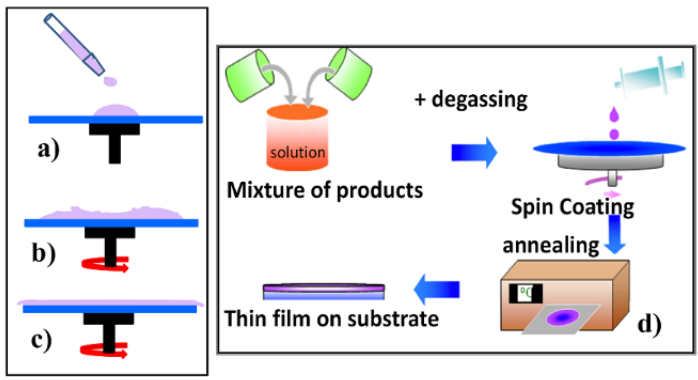

Figure 1.2. *The stages of spin coating technique: a) deposition of volume, b) spreading by rotary spinner, c) homogeneous thin film, d) spin-coating-based manufacturing process. For a color version of this figure, see www.iste.co.uk/dahoo/metrology1.zip*

By spin coating technology, roughness and thickness can be kept under control, their values ranging from about 100 nanometers to several micrometers. Among other factors, the final thickness depends on the concentration of the polymer solution (viscosity) and on the rotational speed

(centrifugal force) of the device. The thickness *d* of a thin film deposited by spin coating is indirectly proportional to the angular speed ω of the spinning plate. It can be written that $d \approx \omega^{-n}$, where the exponent n depends on the solvent. In the absence of evaporation, d varies with time t and speed, such that $d \approx \omega^{-1}t^{-1/2}$ and if the evaporation rate is constant, $d \approx \omega^{-2/3}$. However, it is observed that $d \approx \omega^{-1/2}$. A calibration of the device is required to determine the volume of solution as a function of the desired thickness given the viscosity of the product.

An accurate protocol must be followed before depositing the solutions on the chosen substrate. Quartz (SiO_2) is generally used as a model substrate before trying other substrates that can otherwise be made from ceramics, metal (Al), semiconductor (Si, Ge) or alloy (Cu/Ni, Cu/Ag). Substrates must first be cleaned. If they are not prone to oxidation, an ultrasonic bath is used: the substrate is immersed in water, respecting the allowed volumes between a minimal and a maximal quantity, the bath temperature (T_C: maximum 45°C) and the required time.

There are three stages in a sample preparation: cleaning of the substrate, preparation of the polymer solution to be deposited, then annealing of the polymer.

Surface treatment is essential for avoiding the presence of impurities on the substrate surface. The slightest impurity can generate a contamination that leads to the separation of deposited layers.

– To clean a silicon substrate, an acetone solution at 30°C is used as the ultrasonic bath. After 15 minutes, the wafer is removed from the bath and abundantly rinsed with distilled water followed by ethanol and finally dried by a flow of pressurized dry air. The wafer is then ready to be used as the substrate for the polymer film.

– For a Cu/Ni alloy, the cleaning is done with acetone and distilled water to prevent damage of the nickel layer.

– Quartz or metal (Al) substrates are submitted to ultrasonic cleaning with distilled water and acetone. Each of these baths is applied for 15 min. The substrate is then dried under a flow of pressurized dry air.

Polymer solutions are prepared using a double-barrel syringe with several spare parts. Before the deposition of polymer solutions, it is cleaned by solvents, such as acetone or ethanol. Polymers are generally provided in liquid form of variable viscosity. When the polymer is composed of two components, namely a resin referred to as R and a catalyst referred to as C, R and C must be mixed in a proportion according to the provider specifications (1:1 or 10:1). Since the mixture must be homogeneous, a magnetic stirrer is used for 2 min at 200 rpm for the mixing. Then, several drops are deposited on the substrate using a measuring syringe, before starting the above-described spin-coating process. Programming of the processing steps is set beforehand, depending on the calibration curve of the device. For current polymers, the standard deposition parameters are 1,500 rpm for 55 s and a start ramp of 55 rpm per second. The same deposition conditions are generally maintained for various preparations. The preparation setup is placed under a 30 mbar vacuum for degassing, to prevent bubble formation. This step is carried at ambient temperature.

The next stage after film formation is the curing at a given temperature depending on the polymer to be cross-linked. The cross-linkage mode and the polymer temperature are found in the provider datasheet. If the provided values are respected, a fully polymerized sample can be obtained. In general, if the recommended temperature is exceeded, the material irreversibly deteriorates. Cross-linkage requires a furnace that can heat up to 2,000°C. A degassing chamber comprising a vane pump for low vacuum prevents in a gray room the presence of ambient impurities in the form of dust or aerosol present in the air.

1.2.2. *Physical method: cathode sputtering*

Cathode sputtering (Figure 1.3) involves the bombardment of a target with an inert gas, argon maintained under a reduced pressure ranging between 5 10^{-1} and 10^{-3} Torr, in order to sputter the atoms in the target. It is a mechanical process that depends on the momentum lost by the collider when the Ar^{+} ion collides with the atom in the bombarded target. This process does not depend on temperature. Applying a potential difference between the target (cathode) and the substrate (anode), the sputtered atoms are accelerated and deposit on the substrate. This technique is also known as “sputtering deposition” adequate for thicknesses below 3 µm.

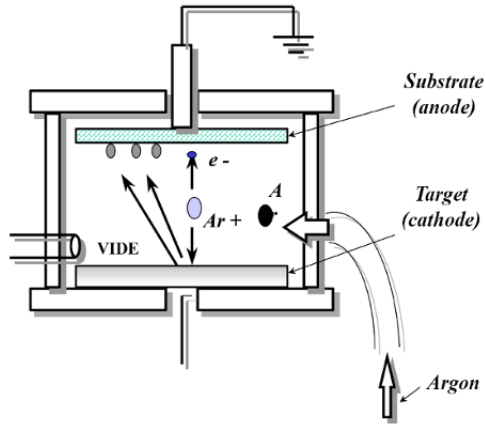

Figure 1.3. *Cathode sputtering. For a color version of this figure, see www.iste.co.uk/dahoo/metrology1.zip*

This technique was used to prepare multi-layers of SiO_2 and TiO_2 films in order to create a 1D magneto-photonic crystal. The target material to be deposited is introduced in a vacuum chamber in the form of a plate of several millimeters thickness and whose dimensions are equal to those of the plate to be coated. This target is fixed at a cathode that is cooled and is maintained under a negative voltage ranging between 3 kV and 5 kV. The anode, which plays the role of the substrate holder, is set in parallel to the target, at a distance of several millimeters. It is generally grounded, for ease of use. For a residual pressure in the chamber maintained between 1 and 10^2 Pa, the electric field between the two electrodes generates the ionization of the visible residual gas in the form of a luminescent plasma cloud. An electric current is then established between the two electrodes, through the conductive plasma formed of electrons, which are attracted by the anode, and positive ions, which are attracted by the target cathode.

A 1D magneto-photonic crystal is a multi-layer stack of a dielectric and a magnetic material characterized by enhanced magneto-photonic properties. The magneto-optical response (Kerr rotation of polarized light) is studied as a function of the thickness of the films by calculation prior to the crystal manufacture and its characterization. The deposition parameters having been calculated, alternating thin films of SiO_2 and TiO_2 are deposited by cathode

sputtering according to the calculated specifications. The criteria to be met are:

– state of the surface: the stacks of dielectric films require the least possible individual roughness of the films to minimize the perturbation generated by this type of defect in the developed structures;

– nature of the material: there should be a significant contrast between the materials to be stacked, with the lowest possible extinction coefficient, which explains the choice of TiO_2 and SiO_2;

– deposition speed: since the development of multilayers requires a significant number of periods, high deposition speeds of single layers are chosen for the stacks over a reasonable period of time;

– deposition temperature: it should be the lowest possible to limit inter-diffusion at the interfaces between SiO_2 and TiO_2 layers.

AFM is used for the study of surface roughness, and ellipsometry is used to determine multilayer thickness and (optical n and k) indices.

The 1D magneto-photonic crystal is thus manufactured using cathode sputtering for multi-layer stacking [HAM 06, HAM 07] and is studied for its properties as smart material at the nanometer scale.

1.2.3. *Physical method: laser ablation*

The principle of thin-film deposition by laser ablation (Pulsed Laser Deposition) involves a nanosecond or femtosecond pulsed laser beam focused on a bulk target (oxide target), in an ultra-high vacuum chamber. The first pulsed laser depositions (PLDs) were conducted in 1965 by Smith and Turner [SMI 65], long before it became widespread, thanks to the development of high-density short-pulse lasers initiated in 1987 [DIJ 87].

The description which is given as an illustration of laser ablation technique concerns the research works conducted at the University of Versailles St Quentin in a laboratory of the National Center for Scientific Research in France for the study of thin films of magnetic oxides of nanometric thickness [DAH 04a, DAH 04, FRA 05, HAM 06, HAM 07, NOU 07]. Two power UV lasers are used: a chemical excimer laser (248 nm) and a solid laser with doubling and tripling crystals. Beyond a certain fluence (amount of energy per unit area or surface energy density),

a light plume can be noted on top of the target. This plume corresponds to a directed expulsion of matter, in the form of a plasma, which can be described as a "gas" of ions, atoms and electrons. These particles are ejected at a high speed while the whole preserves its electrical neutrality. This ejected matter is then collected on a substrate, which is generally a quartz plate located above the target and maintained at a certain deposition temperature. Figure 1.4 shows a schematic representation of the setup corresponding to the laser ablation system.

The samples are prepared in a very high-vacuum chamber under a pressure above 10^{-6} Torr. A light beam from a solid pulsed laser of 10 ns that operates in UV at 385 nm with a repetition rate of 10 Hz is focused on a target that is generally prepared by sintering in the chamber. A reflecting device composed of mirrors that can randomly scan the laser beam on target thanks to an algorithm-based control of the device mirrors is used. The diameter of the laser beam transmitted through a silica window randomly describes a square on the target. Fluence ranges between 2 J/cm^2 and 20 J/cm^2. The substrates (quartz, MgO, etc.) located at the required distance (40 mm to 70 mm) from the target are placed on a holder maintained at an optimal controlled deposition temperature (maximal value of 1,000 ± 5°C) in an oxygen atmosphere under a pressure of up to 500 mTorr.

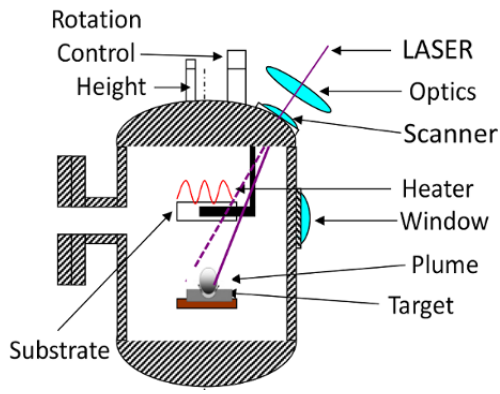

Figure 1.4. *Schematic representation of laser ablation deposition setup. For a color version of this figure, see www.iste.co.uk/dahoo/metrology1.zip*

The solid laser is a flash-pumped Nd: YAG laser. At the output of the laser cavity, a frequency-doubling KDP crystal is used to generate the

second harmonic of laser light at 532 nm. A crystal mixing radiation at 1,064 nm and 532 nm is used to obtain a beam of UV light at 355 nm. Concerning the value of laser radiation fluence at the level of the material, laser radiation–material interaction studies show that it can be classified into three categories:

– Low fluence: the energy deposited by the laser diffuses in the material. It can activate chemical processes at the surface of and/or within the material. The vaporization rate is negligible.

– Intermediate fluence: laser energy is at equilibrium with the losses by heat diffusion and by fusion and vaporization processes. Vaporization is more significant and vapor remains transparent to radiation.

– High fluence: under this regime, a plume appears above the surface of the material, which is generally no longer transparent to laser radiation. Moreover, it may react with the ambient atmosphere and the target material.

The existence of "threshold fluences" beyond which these various phenomena occur can be experimentally observed. They depend on several parameters: radiation wavelength, nature and pressure of the ambient atmosphere and nature and state of the target surface.

A range of parameters can be varied during deposition:

– characteristics of the laser beam: power, beamwidth, duration of the pulse (between 5 and 10 ns for the pulse time at mid-height);

– pressure: between 10^{-4} and 10^{-6} mB;

– temperature of the ceramic heater: between 300 and 800°C;

– oxygen pressure: to maintain the stoichiometry of the sample and confine the plasma. It varies between 60 and 250 mTorr;

– the target–substrate distance: from 40 to 70 mm.

Since the way atoms or molecules are arranged at the surface of a layer determines its morphology and structure, this initial organization plays an essential role in its physical and/or chemical functionalities. Layer growth and morphology optimization is therefore decisive. The growth of layers obtained by laser ablation is achieved by two-dimensional nucleation of aggregates. At a low fluence, these aggregates are small and, in parallel with the subsequent formation of islands, atoms and aggregates scatter at the

surface of the substrate, leading to the formation of layers on top of which aggregates grow. The morphology and structure of layers resulting from this growth mode depend on the conditions of deposition such as the target–substrate geometry, substrate characteristics (surface, nature, temperature), oxygen pressure or the fluence of the ablation laser. Layer growth control involves the optimization of these parameters by in situ controls. As the nature and quality of the deposited layer depend on many parameters (laser energy or fluence, the pressure of the residual gas in the chamber, substrate temperature, etc.), in order to control in situ growth, during deposition, a spectroscopic ellipsometer, as schematically represented in Figure 1.5, was set up in parallel with the preparation system [DAH 03, NOU 07, DAH 11, COA 12]. This non-destructive technique described in Chapter 8 of the [DAH 16] is used to determine layer thickness and optical parameters, i.e. those data required for the analysis of the measurements conducted in magneto-optical spectroscopy.

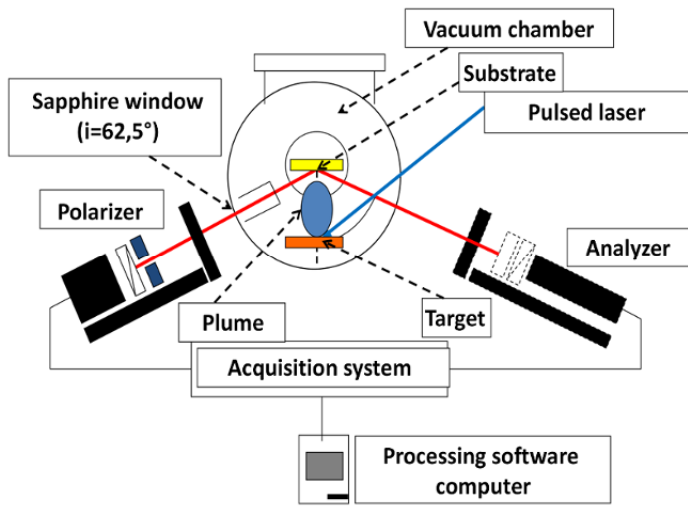

Figure 1.5. *Ellipsometry-based in situ control of thin-film growth. For a color version of this figure, see www.iste.co.uk/dahoo/metrology1.zip*

The results obtained on a thin film of perovskite structure magnetic oxide $SmFeO_3$ deposited on a quartz substrate are given in Figure 1.6(a) and (b) for various temperatures. The ellipsometry parameters cos(Δ) and tan(Ψ) (Chapter 8 of [DAH 16]) are given depending on the wavelength for various temperatures ranging between 300 K and 1,095 K.

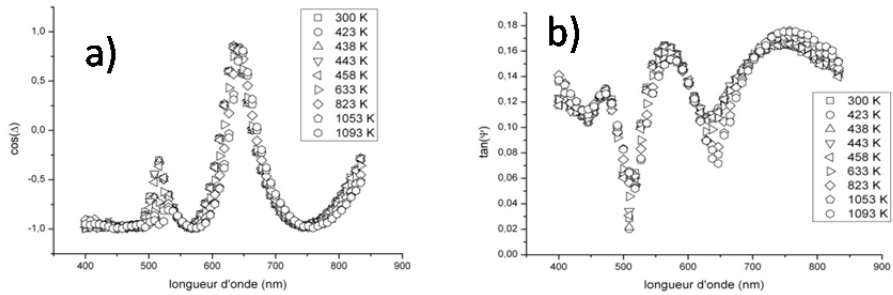

Figure 1.6. *Variation with temperature of a) cos (Δ) and b) tan (Ψ)*

The analysis of the curves shows that beyond 600 nm, cos (Δ) oscillates between ±1, which corresponds to a very low absorption zone. In the absence of thin film, the substrate gives a value of +1 for cos(Δ). When the thin film is deposited, cos(Δ) varies between -1 and +1, the number of oscillations increasing with the thickness of the film. Below 600 nm, in the absorption zone, the maxima remain below 0.1. When temperature increases, varying positions and amplitudes of the extrema can be noted. They shift towards longer wavelengths, which corresponds to an increase in the thickness of the film following the material growth. The amplitudes decrease significantly in the absorption zone, which corresponds to an increase in absorption with temperature. Concerning the parameter tan (Ψ), in the absence of thin film, the quartz substrate gives a ratio of the amplitudes r_p/r_s whose variation is linear in the spectral range from 300 nm to 850 nm, between 0.18 and 0.20. When the film is between the substrate and the air, a variation of tan (Ψ) around this straight line can be noted, with the extrema shifting towards long wavelengths when the thickness increases or the temperature rises. The excursion of the amplitudes, on either side of this line, is a function of thicknesses and absorption.

For the fabrication of a one-dimensional magneto-photonic crystal [HAM 06, HAM 07], the optical properties of TiO_2 and SiO_2 could be determined in the chamber fitted with the ellipsometer, as shown in Figure 1.7. In this case, the target being made of TiO_2, then TiO_2 deposited on SiO_2 could be characterized. The deposition was achieved using an excimer laser that emits a radiation of 248 nm during the discharge triggered by a thyratron in a gaseous mixture of krypton and fluorine. The energy of each pulse, with a duration of about 25 ns, varied over the range from 150 to 650 mJ; fluence

was fixed at 1.8 J/cm^2. Laser repetition rate could be adjusted between 1 Hz and 20 Hz and was fixed at 10 Hz. Substrate temperature was maintained at 300°C, and the pressure of the oxygen in the chamber was measured to be 0.0373 mbar. It is worth noting that laser ablation of SiO_2 at this wavelength is not possible due to an absorption band at 5.01 eV in resonance with the frequency of the excimer laser so that the deposited energy is mainly dissipated by radiative relaxation that manifests as photoluminescence (Figure 6.8 in Chapter 6 of [DAH 16]).

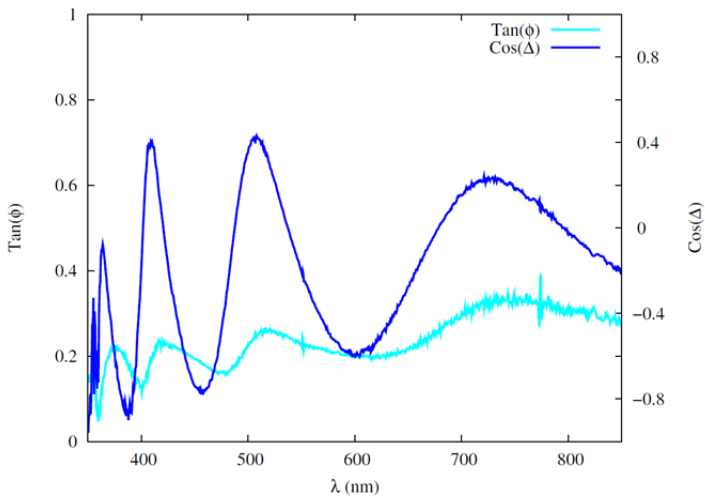

Figure 1.7. *Ellipsometric parameters of a film of TiO_2 on SiO_2 by laser ablation [HAM 07]. For a color version of this figure, see www.iste.co.uk/dahoo/metrology1.zip*

RHEED (reflection high-energy electron diffraction) [RUS 33, COL 72] is generally used as in situ probe to control the growth of thin films. This technique is sensitive to changes at the surface, due to the changes in structure or to adsorption. It involves the bombardment of a target surface with very high-energy electrons. Electrons are then diffracted in various directions with different intensities. The impact of electrons on a phosphor screen gives an image formed of bright spots that correspond to the arrangements of atoms on the surface. A beam of accelerated electrons (5–100 keV) under grazing incidence (0.5 to < 3 deg) is reflected on a surface. Due to their energy, the penetration of electrons is significant. But because of the grazing incidence, only few atom layers are probed. Hence, this technique is sensitive to surfaces.

Two types of diffraction are possible: by reflection and by transmission–reflection: 1) diffusion by a 3D crystal island (image in the upper part of the screen); 2) 2D surface diffusion by a plane surface (image in the lower part of the screen). The energy of electrons in a RHEED experiment may vary between 10 keV and 100 keV, but most of the instruments use energy between 10 keV and 35 keV. Let us recall that 1 eV is the kinetic energy gained by an electron that is accelerated under a potential difference of 1 V. The kinetic energy is $E_c = 1/2\ mv^2$, where v is the speed of the electron and the electric energy is expressed in eV. The speed is $v = \sqrt{(2eV/m)}$ and using the momentum $p = mv$ and the de Broglie relation $p = h/\lambda$, it can be deduced that $\lambda = h/\sqrt{(2meV)} = \lambda_c$ for a non-relativistic electron. Under relativistic conditions, when energies are high, mass correction must be taken into account, and therefore $\lambda = \lambda_c(1/\sqrt{(1 + eV/2mc^2)})$. The corresponding wavelength varies between 0.0037 nm and 0.0146 nm for energies of 100 keV and 10 keV.

1.3. Characterization of samples

A thin film of a given material is an amount of that material having one of its dimensions, referred to as thickness, significantly reduced. This thickness (in nanometers) corresponds to the distance between two boundary surfaces (quasi bi-dimensionality). This 2D structure results in a perturbation of most of its physical properties. The essential difference with the bulk state is that the role played by the boundaries in the bulk properties is generally considered negligible. On the other hand, in a thin film, the effects related to boundary surfaces are predominant. The smaller the thickness, the more pronounced is this bi-dimensionality effect. Conversely, beyond a certain threshold, the effect of thickness becomes negligible and the material regains its properties of the bulk material. Any method of analysis requires a probe (electromagnetic radiation, a beam of energetic particles, a field, a mechanical penetrator, etc.) acting on a sample. The result of the interaction between this probe and the sample can be another radiation, particles, field variation, detected by a chain of measurement or by a behavior law.

To observe small-sized objects, a microscope equipped with lenses is used in order to realize a magnification of the object when it is viewed through the objective of the apparatus. The object must be illuminated, which is done either by reflection or by transmission, the light reflected or scattered by the object being then recovered by the objective, which forms

an image that can be observed. It is in 1873 that E. Abbe [ABB 73] formulated his mathematical theory concerning images formed by a microscope and showed that a point could not be imaged by a point. While working on the theory, he identified a limit to the size of the observable object, which was due to the resolution $d = 0.61\lambda/ NA$, where the numerical aperture is $NA = 2n\sin\alpha$. It is expressed as a function of the maximal angle α between the optical axis and the rays coming from the object viewed through the objective under which various rays lead to the formation of the image of the object; n is the refractive index of the environment in which the object is immersed. This resolution limit is nowadays known as the Rayleigh criterion and is associated with the wavelength λ of the radiation used for the observation. It is due to interference effects that lead to the formation of the Airy disk, which for an aperture of diameter D is given by $1.22\lambda/D$ under incoherent illumination. The same phenomenon accounts for the "waist" present in the Fabry–Pérot setup used in a laser device, as described in Chapter 6 of [DAH 16] (Figure 6.2). Resolution is limited to 200 nm in the visible spectrum. Abbe thought however that this limit could be overcome with the forthcoming progress in the understanding of physical phenomena or technology.

Indeed, around 55 years later, in 1928, E.H. Synge [SYN 28] proposed a thought experiment that laid the bases of near-field microscopy of modern optics, considering that it was possible to obtain resolutions beyond the limits imposed by diffraction. He considered that it was possible to observe by transmission the interaction of light and matter between an object and the light that would reach the object through a small aperture of dimensions smaller than the wavelength, of the order of 50 nm to 100 nm, in a screen that scans the surface of the object, as shown in Figure 1.8. Using this method, the limit of resolution is no longer imposed by the wavelength, but by the aperture through which light passes. In the theory of light diffraction through a small aperture, the components of the far field can propagate, while in the near field, they are evanescent (see the Appendix: Propagation of a Light Ray). In the proximity of the object, spatial frequencies are high. Referring to the works of Fresnel and to Babinet's theorem, a small-size aperture being equivalent to an object of the same dimension from the perspective of diffraction, this principle prefigures the use of a tip to probe the evanescent waves near a surface.

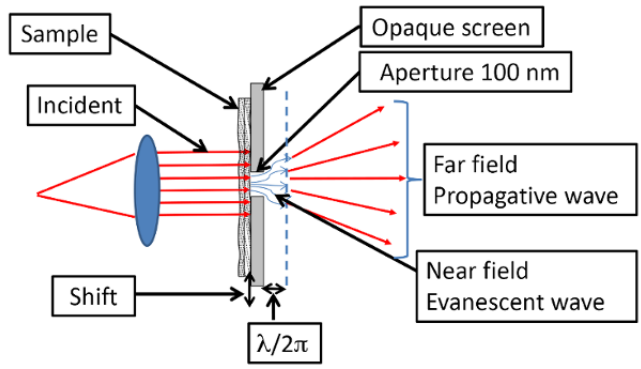

Figure 1.8. *E.H. Synge experimental setup. For a color version of this figure, see www.iste.co.uk/dahoo/metrology1.zip*

Similar to nanotechnologies, it took a while for the idea to be put into practice. In this case, four decades were needed to obtain a better resolution with a scanning microscope developed in 1972 [ASH 72], in the domain of microwaves with a wavelength of 3 cm. A grating could be resolved with a resolution of $\lambda/60$ by this technique.

But meanwhile, scanning tunneling microscope (STM) was invented by Binnig and Roher in 1981 [BIN 82a, BIN 82b, BIN 83, BIN 86a]. The operating principle of STM, which uses the scanning method, relies on the possibility to establish a tunneling current between a metal tip and a metal or conductive surface when a potential difference is maintained between the tip and the surface. The intensity of this current depends on the distance between the tip and the surface. When the tip scans the surface, there is a variation of the distance between the surface and the tip due to surface topology, and consequently the tunnel current, which depends on this distance, also varies. In this case, the current variation is a measure of the surface topology. A second operating mode involves maintaining a constant distance between the surface and the tip. Taking a starting point as a reference, a rated current is fixed. Given that the current variation is positive when the distance between the tip and the surface decreases, and that it is negative when the distance increases, this variation is injected into a feedback system (negative feedback loop) in order to maintain a distance that is equal to the reference distance. The positive or negative correction of the position, made by moving the tip using a piezoelectric system [SYN 32] that expands or contracts when subjected to a potential difference (see Chapter 7 on

intelligent materials), is in this case directly related to the topography of the surface. It is worth noting that nowadays STM belongs to the class known as scanning probe microscopy (SPM), but its use is limited to electrically conductive materials.

Finally, in 1984, the first near-field optical microscope is developed [POH 84] in the visible spectrum. The operating principle of scanning near-field optical microscope (SNOM) or near-field optical scanning microscope (NSOM) relies on the Synge principle, but uses an STM, with a probe instead of an opaque screen with an aperture, that is localized in the near-field zone. At nanometric distances, the movement of the probe on a surface is in fact easier to control than that of an opaque plate with an aperture.

A brief description of a SNOM by transmission is provided, as schematically represented in Figures 1.9. and 1.10, highlighting the main elements required for its operation. In a typical optical setup, a laser beam, after passing through neutral filters, is collimated, so that the light rays are quasi-parallel, which corresponds to the propagation of a plane wave (Figure 6.2, Chapter 6 of [DAH 16]). It is then directed under the acceptance angle in an optical fiber whose tip end is near the surface to be analyzed. An optical system is used to recover the signals collected in near field on an APD (Avalanche Photo diode) detector for an analysis through a spectrometer and a processing software. The main elements contributing to data collection are the tip-shaped probe and the precise measurement of the probe movement with respect to the sample by means of a piezoelectric plate subjected to a potential difference. The latter which drives the tip along X, Y or Z is a function of the error signal generated by the laser detection system with a PSD (Position Sensitive Detector) quadrant, which gives the tip position with respect to the surface during the lateral scanning generated by the piezo stage. This scanning is in raster mode, similar to the scanning mode on a television screen. The feedback loop system operates in two modes: at constant force or at shearing force.

In Figure 1.9, the setup of the piezo stage corresponds to the constant force mode. In this case, scanning can be conducted in 3 modes. The contact mode corresponds to the situation in which the tip touches the surface of the sample and maps the topography of the surface. In this mode, there is a risk of sample damage. The tapping mode corresponds to a flexible tip that undergoes deflection according to the topography of the surface. The laser-PSD system measures the deflection angle and generates an error

signal, which is used to activate the piezo stage by the feedback loop in order to bring the surface to the reference nominal distance. Finally, the non-contact mode corresponds to that of a high-frequency generator being associated with the tip under oscillation. The amplitudes of these oscillations are modified according to the topography of the surface, and depending on whether the surface gets closer or farther, the vibrations are damped or relaxed by long-range (dispersion) forces between the surface and the tip. Depending on the decrease or increase in vibration amplitudes, the feedback system modifies the distance between the tip and the surface.

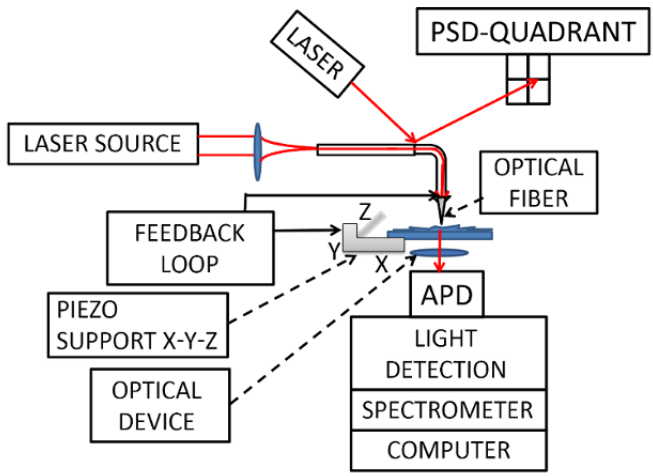

Figure 1.9. *Diagram of a SNOM by transmission in constant force mode. For a color version of this figure, see www.iste.co.uk/dahoo/metrology1.zip*

Another possible setup is that of the tip-carrying fiber being attached to a tuning fork, which sets the tip in a lateral vibration movement above the surface (Figure 1.10). In this shearing force mode, the positioning principle is similar to the above-described contactless mode. Hence, similar to an STM that gives the possibility to probe the metallic surfaces at nanometer scale, the near-field optical microscopy can be used to reach sub-wavelength resolution. A local probe detects a non-radiative signal confined in the close vicinity of the surface, similar to the tunnel current, which is active on the sample surface. Since the probe scans the sample surface at a distance or height of several nanometers, similar to the STM, a negative feedback loop is used to follow the topography of the surface.

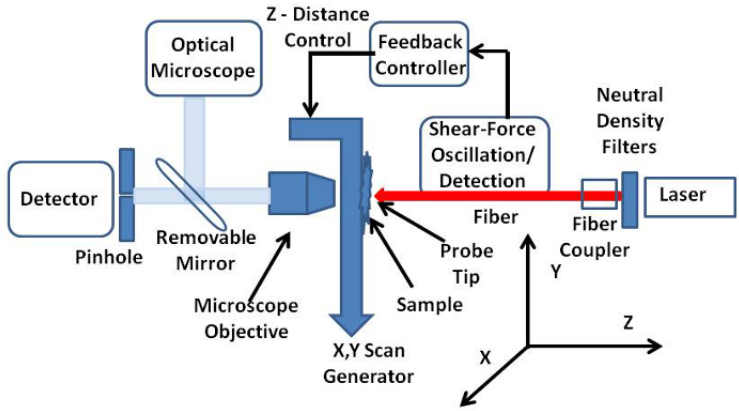

Figure 1.10. *Diagram of transmission SNOM in shear mode. For a color version of this figure, see www.iste.co.uk/dahoo/metrology1.zip*

The atomic force microscope (AFM) was invented in 1986 by Binning, Quate and Gerber [BIN 86b] in a collaboration between IBM and Stanford University. A more detailed discussion on the use of this instrument is provided in the study of thin films of magnetic oxides prepared by laser ablation in section 1.3.2.

In summary, the types of microscopes commonly used nowadays correspond to tunneling and atomic force near-field microscopes, referred to as STM and AFM, respectively. The very high spatial resolution characterizing near-field techniques is related to the very small size of the probe – in the two cases considered, the nanometric apex of a conductive or semi-conductive metallic tip brought to near-contact (a fraction of nanometer) with the surface of the sample. These microscopes use the localized interactions of the tip with the sample and their rapid variation of intensity with the probe–sample distance: the passage of the tunneling current for the STM from which a mapping of the surface atoms is obtained through their local electronic density, and the forces acting on the tip (e.g. Van der Waals interactions for the AFM).

These near-field microscopies give also access to further information, such as electronic spectroscopy by STM and mapping of force fields for AFM and its homologues. The downside of the spatial resolution of these microscopies is the limitation of the analysis to the surface of the sample and

to the zones of limited dimension, STM use being also limited to the study of conductive samples. Moreover, the probe may have an invasive effect.

It is worth noting that optical microscopy in the context of light–matter interaction can also be implemented in far field, being in fact less invasive and making it possible to observe (imaging, localization, detection) the sample. Moreover, many spectroscopic signatures can be studied through various spectroscopies using a classical source or a laser as source (Chapter 6, [DAH 16]) such as Brillouin or Rayleigh scattering, absorption or emission spectroscopy (fluorescence or phosphorescence) or Raman spectroscopy, the pump-probe spectroscopy, the double resonance used for probing the properties of matter through the various sub-structures of its energy levels. This spectroscopic analysis can be further extended to the acquisition of physical and chemical parameters such as the lifetime of electronic states. The reader who is interested in the developments of these techniques can refer to the list of references [LEW 833, BET 86, BET 87, FIS 88, COU 89, RED 89].

1.3.1. *Scanning electron microscope*

Electron microscopes are based on the wave–particle duality of the electron Reducing the wavelength of the radiation provides a better resolution than conventional optical microscope. Historically, the first revolution in the field of very high-resolution imaging is that of scanning and transmission electron microscopies (SEM and TEM) (RUSKA 1931), which provide images with nanometer and even atomic resolution due to the nanometer dimension of the electron beam for SEM. Electron microscopy is a very powerful tool, which can also be coupled with spectroscopic chemical analyzes (EELS: electron energy loss spectroscopy) in TEM and structural (diffraction) but their implementation remains very limited, and Electron microscopy is also now widely and mainly used as an imaging tool.

The scanning electron microscope (SEM) relies on the wave properties of an electron to obtain magnification. Figure 1.11 shows the schematic representation of an electron microscope in TEM and SEM modes.

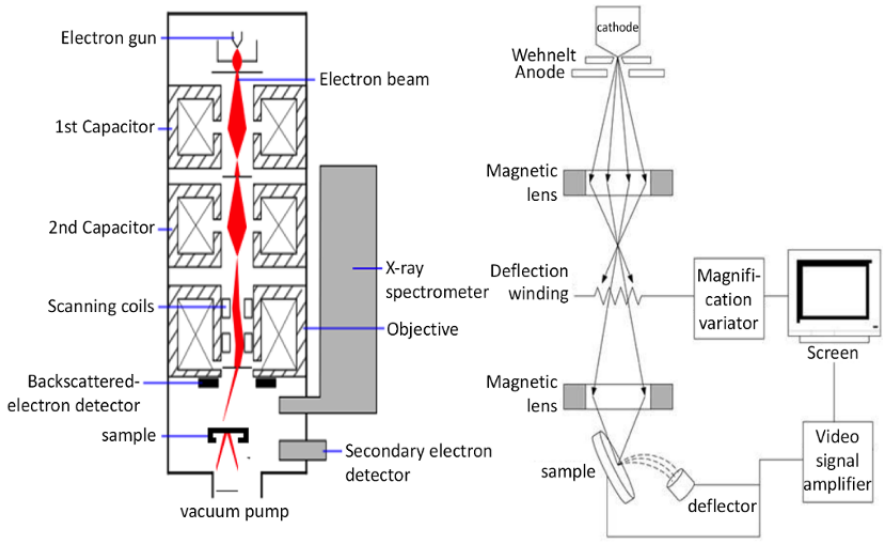

Figure 1.11. *Electron microscope: TEM and MEB modes. For a color version of this figure, see www.iste.co.uk/dahoo/metrology1.zip*

A beam of mono-kinetic electrons is produced by a tungsten filament through which a current is generated by the thermionic effect. Electrons are accelerated by a potential difference V of the order of 100 keV. The wavelength λ associated with electrons is given by the de Broglie relation, $\lambda = h/(\sqrt{2m_e eV})$, where m_e designates the mass of the electron and e its charge. Under 100 keV, the electron wavelength λ is 0.0037 nm. This beam is directed and focused by magnetic lenses to obtain a very small-diameter probe (about 0.01 µm) that scans the surface of the studied sample. Because electrons penetrate the material, the resolution is however not good (rather of the order of a micron for backscattered electrons and of the order of several tenths of a micron for secondary electrons). Electron scattering through the studied sample can be either elastic (no energy loss upon interaction with the nucleus and electrons inside the atoms), which leads to diffraction or plastic (effect of heterogeneities such as grain material boundaries, dislocations, defects, density variations, etc.), which leads to a variation in the intensity of the transmitted beam. The two modes of operation of a TEM are the image mode and the diffraction mode.

The interaction between the beam of electrons and the material generates various types of radiation:

– backscattered electrons;

– secondary electrons;

– absorption generating a current in the sample;

– Auger electrons related to atom de-excitation;

– X-rays emitted during de-excitation following the ionization of electron shells inside the atoms.

The studies of thin films of magnetic oxides were conducted with a Philips CM20 TEM and a Jeol 200CX TEM operating at 200 kV. The two instruments were equipped with a sample support that could be tilted along two axes. Adjustments were directly made on the image displayed by the screen of the image intensifier. Sample preparation involves thin-film manufacturing by ion bombardment perpendicular to the surface (section of the plates). Due to the ion tendency to melt the material, a proper control of this stage is required to avoid sample damage. For the analysis of sections, the surfaces of two pieces of epitaxial layers are glued with epoxy. The section is then mechanically polished on both sides until reaching a thickness of 30 μm and then carefully thinned down by a flow of low-speed argon ions on the samples (6 kV and 10 mA) on a liquid nitrogen-cooled support. This process prevents damages. A surface of the order of 20 μm^2 can then be analyzed by TEM [DAH 04a]. Figures 1.12(a) and (b) and 1.13(a) and (b) show images obtained by TEM for $SmFeO_3$ materials deposited at 785°C and 820°C, respectively.

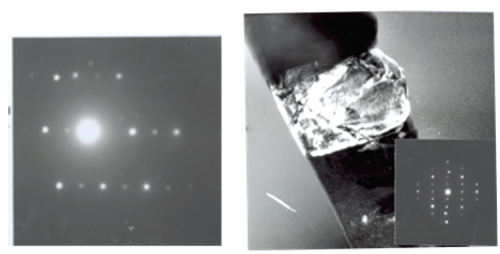

Figure 1.12. *Diffraction images obtained by TEM for SmFeO3 samples deposited at: a) 785°C and b) 820°C*

TEM-based diffraction analysis reveals two types of structures depending on the temperature deposition of the $SmFeO_3$ film on a quartz substrate: a cubic structure (Figure 1.13(a)) and an orthorhombic structure (Figure 1.13(b)). The deposition has a columnar form in volume with surface extrusions, as shown in Figure 1.12(b) and Figure 1.13(a) and (b).

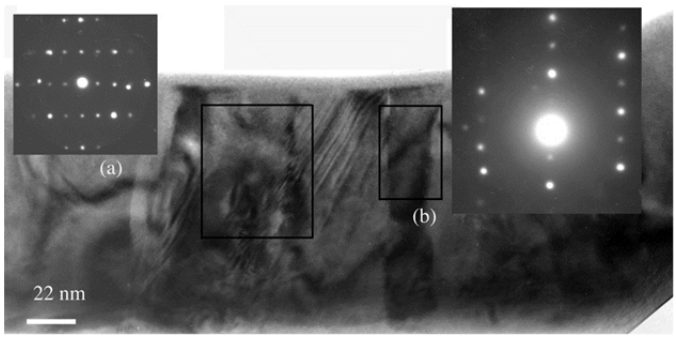

Figure 1.13. *TEM diffraction images for SmFeO3 films deposited at: a) 785°C and b) 820°C*

Figure 1.14(a) and (b) displays SEM images of $SmFeO_3$ films deposited on a quartz substrate at a temperature of 915 C. It is worth noting the presence of protuberances whose dimensions range between 150 and 500 nm, as observed in TEM, and cracks due to different expansion coefficients of the substrate and of the oxide layer, ranging between 50 and 90 nm.

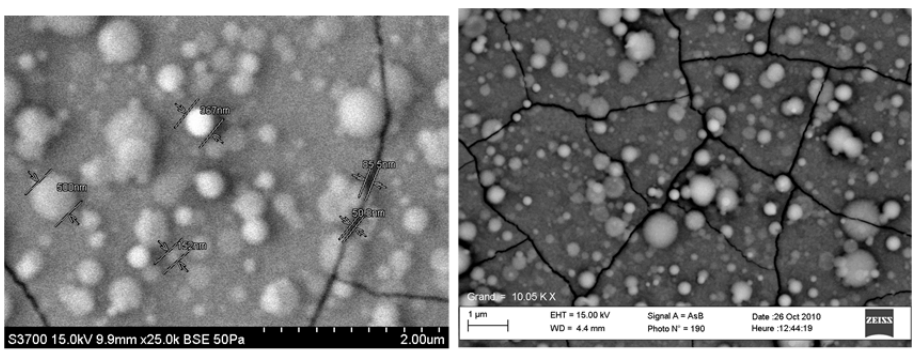

a) (b)

Figure 1.14. *SmFeO film deposited at TD = 915°C: a) protuberances between 150 and 500 nm; b) cracks between 50 and 90 nm*

1.3.2. *Atomic force microscope*

The atomic force microscope (AFM) is used to obtain three-dimensional analyses of layer roughness with a good vertical resolution. Its operating principle is represented in Figure 1.15 and involves the measurement of the variations of forces of interaction between a tip and the surface under study.

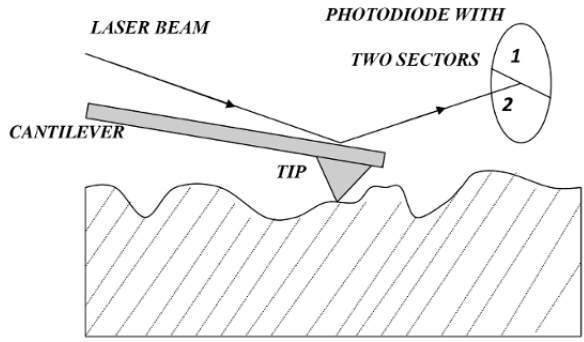

Figure 1.15. *AFM operating principle*

An atomic force microscope is constituted of a piezoelectric quartz plate on which the sample to be studied is placed. The quartz plate lies on an "elevator" engine, and above the sample, there is a very hard tip (read head) fixed at the end of a beam in a frame. A laser beam is reflected on the tip and illuminates two photodiodes. The tip tilt on the scanned surface is determined by the difference in light intensity on the photodiodes. The variation of this electrical signal when the plate under the tip is under translational motion is processed by a software that consequently deduces the topography of the scanned surface.

Figure 1.16 shows the various constituents of an AFM microscope:

– The tip: made from silicon nitride, it is the finest possible, with a pyramid shape.

– The engine: its main role is to lift the sample towards the tip.

– The quartz: it is first of all used for the precise adjustment of the tip on the deposition. Due to the voltage across it (due to the crushing of the tip), it can be used for the computer representation of the deposition surface. Two other voltages are applied to it in order to move the sample in the two directions of the plane.

– The laser: it has a low power – its maximal power is 5 mW. Its essential characteristic is the beam fineness. It emits light in the red band with a wavelength of 670 nm.

– The photodiodes: they generate an electrical signal that is proportional to their respective illumination and thus serve as "sensor of approach" of the tip to the deposit.

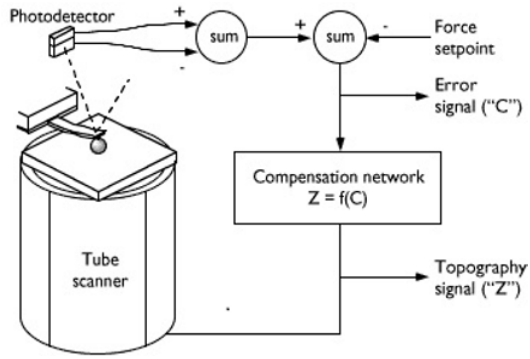

Figure 1.16. *Atomic force microscope*

The work is conducted in the contact mode, the forces being measured in the short range "repulsive" mode.

The laser beam is directed to a metallized part of the cantilever that scans the sample surface horizontally. Due to the deflection of the cantilever, the forces between the tip and the surface can be obtained by the deviation of a laser beam reflected on the metallized part of the cantilever and measured by a quadrant diode (1 and 2). The position of the sample is adjusted along the vertical axis depending on the signal on the diode. Prior to starting a measurement, the laser beam illuminates each quadrant with the same intensity (Itot = I1 - I2 = 0). A vertical variation of the tip position leads to a shift of the beam on the detector and the appearance of the measurement signal (Itot $\neq$ 0). The signal Itot is then used to vary the position of the piezo-electric engine in order to bring the cantilever to the initial position (Itot = 0). The recorded scanning traces are processed and transformed by a special software into three-dimensional images representing the studied surface.

There are several artifacts for surface measurement with AFM. The most inconvenient in the case of thin films are real geometry and the radius of curvature of the tip, as well as the inertia of the feedback of the piezo-electric engine in case of very high roughness. Since a measurement is the result of a convolution between the geometry of the tip and the irregularities of the surface, the shape of the grains observed on an AFM image is not always actual. To avoid the effect of this artifact, scanning under several angles is recommended. The lateral resolution of an AFM image depends on several factors, among which is the morphology of the surface (notably the size of the grains, their amount and the distance between neighboring grains) and the radius of curvature r_c of a tip. For the tip with r_c = 50 nm, the lateral resolution for two grains of height 20 nm is 38 nm. This means that, in order to optically resolve these two grains, the distance between them should be greater than or equal to 38 nm.

The algorithm analyzing the roughness of the film surface is the following: first, a scanning of the maximal possible surface (10 × 10 μm) is conducted, then, if needed, a zone without large grains or agglomerates (scanning surface typically 800 × 800 nm) is chosen and roughness is studied. After having repeated this process several times on different areas of a layer, the mean value of the roughness and the mean size of the grains for polycrystalline layers are obtained.

Images of 2 × 2 μm surfaces on samples deposited under an oxygen pressure of 50 mTorr are displayed in Figure 1.17(a)–(c). Disk- or square-shaped islands of spherical, cylindrical or cubic morphology are observed below the layers deposited at 510°C, 635°C and 755°C. Inspection shows that the size of these islands is smaller at 755°C. The roughness determined on the surfaces of 2 × 2 μm and 10 × 10 μm surfaces is in agreement with the roughness obtained by TEM and SE (spectroscopic ellipsometry) [DAH 04a]. The analysis of AFM images of the samples deposited under three different oxygen pressures (24 mTorr, 52 mTorr and 62 mTorr) are displayed in Figure 1.18(a)–(c), for a temperature of deposition of 920°C. Islands of various forms are also observed, their size being smaller when the pressure is lower. Roughness values between 10 and 30 nm are compared to those determined by TEM and SE [DAH 04a].

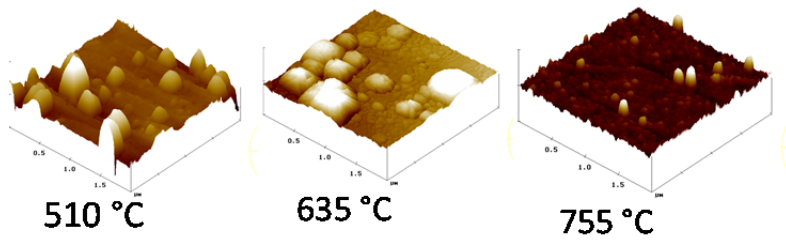

Figure 1.17. *Topology of the deposition surfaces of $SmFeO_3$ on quartz (P = 50 mTorr) for various deposition temperatures. For a color version of this figure, see www.iste.co.uk/dahoo/metrology1.zip*

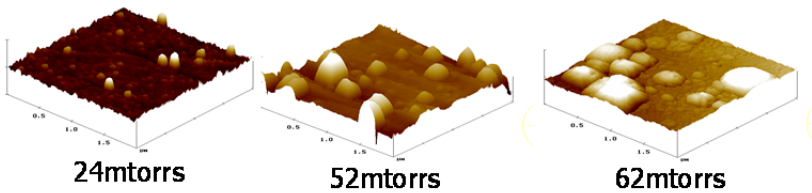

Figure 1.18. *Topology of deposition surfaces of $SmFeO_3$ on quartz (T = 920°C) for various oxygen pressures. For a color version of this figure, see www.iste.co.uk/dahoo/metrology1.zip*

1.3.3. *Infrared spectroscopy (FTIR/ATR)*

Infrared spectroscopy is used to study the vibrational and rotational motions of molecules in the gaseous phase [DAH 17, DAH 19, DAH 21] and also the vibrational motion of molecules in the condensed phase. Modern characterization instruments rely on the principle of spectroscopic interferometry. It is a non-destructive technique. It can be applied to study the vibration modes of molecules in the medium-infrared-energy domain of polymer materials prepared by spin coating. The identified modes of vibration are used to determine the nature of the chemical bonds susceptible to be present in the molecule. The position (wavelength) and intensity (% in height or surface of the rays) of absorption peaks are specific for various chemical groups. The medium-infrared domain corresponds to the interval 400 $cm^{-1} < \sigma$ (wave number) < 4,000 cm^{-1}.